REVIEW OF RESEARCH

FABRICATION OF POLYCRYSTALLINE $Ni_{0.5}Co_{0.5}Fe_{2-x}Pr_xO_4$ NANOPARTICLES AND THEIR STRUCTURAL INVESTIGATIONS

Kadam V. B.[1], Jadhav Govind[2], Kirti Desai[3], Swati Patil[4], N. D. Shinde[1]

[1] Chemistry Department, Shivaji College, Omerga, Dist. Osmanabad (M.S.) India .
[2]Physics Department, Shivaji College, Omerga, Dist. Osmanabad (M.S.) India .
[3]Physics Department, A.S.C. College, Dharur (K), Dist. Beed (M.S.) India.
[4]Physics Department, Pratapsinh Mohite College, karmalla, Dist. Solapur (M.S.) India.

ISSN: 2249-894X
IMPACT FACTOR : 5.7631(UIF)
UGC APPROVED JOURNAL NO. 48514
VOLUME - 8 | ISSUE - 8 | MAY - 2019

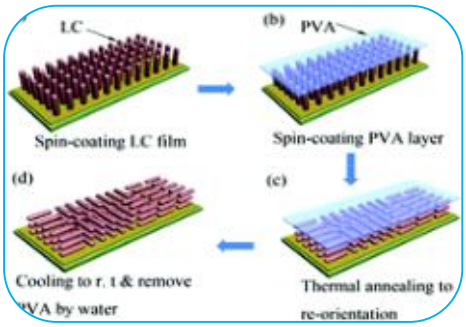

ABSTRACT:

Nanocrystlline ferrite powders of the series $Ni_{0.5}Co_{0.5}Fe_{2-x}Pr_xO_4$ (x = 0.0, 0.025, 0.050, 0.075, 0.1) prepared via sol-gel auto-combustion route were characterized by x-ray diffraction technique for the detailed structural investigations. The samples are obtained at relatively low sintering temperature of 700^{0}C for 4h. The structure of the samples was confirmed by using X-ray diffraction technique and other related parameters are also evaluated such as lattice constant, X-ray density, and particle size and cation distribution. Samples possesses single phase cubic spinel structure with lattice constant lies between 8.35 – 8.39 Å. Particle size obtained from the XRD data shows decreasing trend with the addition of Pr^{3+} ions. The hopping lengths 'L_A' and 'L_B' were calculated from the values of lattice constant. The values of hopping lengths increase with increase in Pr content 'x'. The cations distribution suggests that the Fe^{3+} and Pr^{3+} cations are distributed randomly over tetrahedral – A and octahedral – B sites where as Co^{2+} ions shows strong preference towards octahedral – B site.

KEYWORDS: *Nanocrystalline, lattice parameter, cation distribution.*

INTRODUCTION

Polycrystalline ferrite nanoparticles are attracting many researchers as they are having wide range of applications in various fields. Ferrites are very good dielectric materials, as the preparation of ferrite powders is possible in polycrystalline form. The properties of ferrites are very sensitive to synthesis methods, amount and type of dopants. The impurity addition dramatically changes the structural and physical properties of ferrites. In chemical methods of preparation of ferrite particles with nanosize dimensions having desired physical properties, the structural and chemical properties of constituent ions are of prime importance [1]. In the last few decades significant work has been reported on the pure and substituted spinel ferrites because of their theoretical and technological importance [2-4]. Among the all classes of ferrites, Ni ferrites possess inverse spinel structure. Substituted nickel ferrites have high Curie temperature and cobalt ferrites are having high coercivity. The synthesis of doped nickel and cobalt ferrite nanoparticles has been investigated due to their wide range of applications in various fields [5-7].

In the present work, the structural properties of Pr doped Ni-Co-Fe-O ferrite system synthesized by sol-gel auto combustion technique will be investigated. The structural properties are investigated by using X-ray diffraction.

EXPERIMENTAL:

Sample Preparation:

Pr doped Ni-Co ferrite system with general chemical formula $Ni_{0.5}Co_{0.5}Fe_{2-x}Pr_xO_4$ (with x = 0.0, 0.025, 0.050, 0.075, 0.1) is prepared by sol-gel auto combustion method. Nickel Nitrate $(Ni(NO_3)_2.6H_2O)$, Cobalt Nitrate $(Co(NO_3)_2.6H_2O)$, Ferric Nitrate $(Fe(NO_3)_3.9H_2O)$, Presidium Nitrate $(PrNO_3)_3.9H_2O)$ are taken as starting materials (A.R. grade) with high purity (98.5 %). All the nitrates are dissolved in distilled water with their weight proportion. Citric acid $(C_6H_8O_7{\cdot}H_2O)$ is used as chelating agent and added to the nitrate solution with molar ratio of 1:3. To adjust the pH ≅ 7, liquid ammonia is poured slowly to the nitrate solution. The whole mixture is subjected towards magnetic stirrer with hot plate for continuous stirring at constant temperature 80^0C. After 2-3 hours of constant heating and stirring, the mixture is converted in to gel and thereafter gets self ignited and burnt. The burnt powder is sintered at 700^0C for 4 hours as to obtain the final product.

Characterization:

All the samples of the series $Ni_{0.5}Co_{0.5}Fe_{2-x}Pr_xO_4$ with x = 0.0, 0.025, 0.050, 0.075, 0.1 are characterized by various techniques in order to get information regarding structural, magnetic and electrical properties. To obtain the exact sintering temperature, a thermo gravimetric analysis (TGA) is carried out for a typical sample. The TG study is carried out by using Shimadzu DT-40 automatic thermal analyzer in the temperature range of 100^0C to 900^0C. Room temperature X-ray diffraction technique (Regaku *(Miniflux II)* diffractometer) is used to obtain the X-ray diffraction data of all the samples. Cu-K_α radiations (λ = 1.5406 Å) at 40kV are used for X-ray diffraction in the 2θ range of 20^0 to 80^0 and the scanning rate is maintained at 2^0 per minute.

RESULTS AND DISCUSSION:

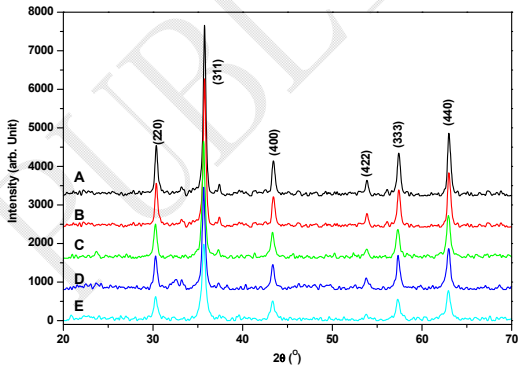

Figure 1: XRD plots of $Ni_{0.5}Co_{0.5}Fe_{2-x}Pr_xO_4$ ferrite system (A: x = 0.0, B: x = 0.025, C: x = 0.050, D: x = 0.075 and E: x = 0.1)

Room temperature X-ray diffraction patterns of all the samples are shown in Figure 1. The reflections are occurred for the main planes (220), (311), (400), (422), (333) and (440). From the reflection pattern shown in Figure 1, it is clear that all the planes are indexed and confirms the single phase cubic spinel structure. Absence of impurity peak confirms the homogeneity of the samples. The XRD data is used to estimate the structural parameters viz. lattice parameter, particle size, X-ray density, porosity and cation distribution. The values of lattice parameter have been calculated by using miller indices and interplanner spacing of the respective planes. Pr^{3+} substitution in Ni-Co ferrite increases the lattice parameter and the calculated values are ranges from 8.3500Å to 8.3862Å.

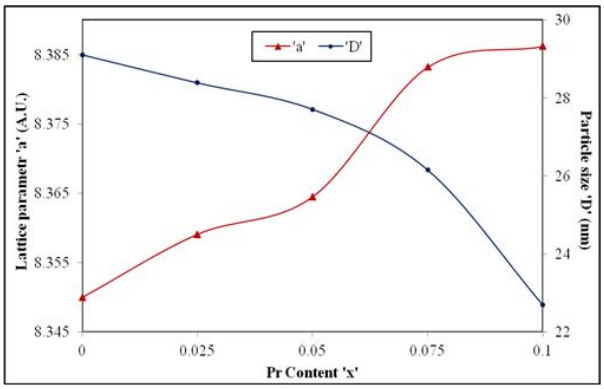

Figure 2: Variation of lattice parameter 'a' and particle size 'D' with Pr content 'x' in $Ni_{0.5}Co_{0.5}Fe_{2-x}Pr_xO_4$

Figure 2 shows the graphical variation of lattice parameter as a function of Pr content 'x' and the calculated values are given in Table 1. The variation of lattice parameter is related to the difference in ionic radii of the metal ions which are exchanged with each other. Here, in this case, Fe^{3+} ions having radii 0.67Å are replaced by Pr^{3+} ions having ionic radii 1.13Å. Increase in ionic radii increases the cell volume and in results increases the lattice parameter. The unit cell volume of all the samples is calculated by using following relation [8];

$$V_{cell} = a^3 \qquad 1$$

where, 'a' is the lattice parameter and the calculated values are listed in Table 1. It is observed from Table 1, that the unit cell volume increases with increase in Pr concentration and the values are lies in the range 582.18 - 589.79.

Table 1: Lattice parameter 'a', Unit cell volume 'V', crystalline size 'D_{xrd}' , X-ray density (d_X), bulk density (d_B), percentage porosity (P), specific surface area (S) and hoping lengths (L_A and L_B) for $Ni_{0.5}Co_{0.5}Fe_{2-x}Pr_xO_4$ ferrite system.

'x'	'a' (Å)	'V' (Å³)	'D' (nm)	'd_X' (g/cm³)	'd_B' (g/cm³)	'P' (%)	'S'	'L_A' (Å)	'L_B' (Å)
0.0	8.3500	582.18	29.11	5.3513	4.2630	25.52	48.35	3.616	2.952
0.025	8.3591	584.09	28.39	5.3822	4.2763	25.86	49.42	3.620	2.955
0.050	8.3645	585.22	27.71	5.4200	4.2871	26.42	50.50	3.622	2.957
0.075	8.3832	589.15	26.16	5.4318	4.2924	26.54	53.44	3.630	2.964
0.1	8.3862	589.79	22.70	5.4739	4.3174	26.78	61.22	3.631	2.965

The average particle size 'D' is calculated by using the broadening of most intense diffraction peak (311) using the well known Debye Scherrer relation [9];

$$D = \frac{0.9\lambda}{\beta \mathrm{Cos}\theta_B} \qquad 2$$

where, 'D' is average particle size, 'λ' is the wavelength of incident radiation, 'β' is the Full Width of Half Maxima (FWHM) and θ_B is the Bragg's angle. Table 1 shows the values of particle size obtained from XRD data and the variation is shown in Figure 2. It is observed that the particle size decreases

from 29.11 nm to 22.70 nm. The X-ray density 'd_X' is calculated by putting the values of molecular weight and lattice constant and the values are given in Table 1. It is clear that the X-ray density increases with increase in Pr content 'x'.

The bulk density 'd_B' of all the samples is obtained by simple mass – volume relation. The calculated values of bulk density are given in Table 1. The bulk density is found to increase with increasing Pr content 'x'. For the series $Ni_{0.5}Co_{0.5}Fe_{2-x}Pr_xO_4$ both molecular weight and cell volume increases, hence the bulk density increases. The percentage porosity 'P' of all the samples of the series $Ni_{0.5}Co_{0.5}Fe_{2-x}Pr_xO_4$ is calculated by using the relation discussed elsewhere [10].

Hopping lengths 'L_A' and 'L_B' (distance between magnetic ions) are calculated by using the following relations [11],

$$L_A = a\sqrt{\frac{3}{4}} \qquad 3$$

$$L_B = a\sqrt{\frac{2}{4}} \qquad 4$$

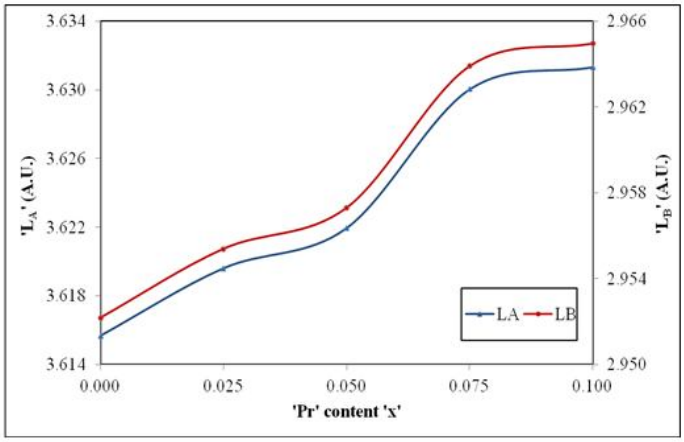

Figure 3: Variation of hopping length 'L_A' and 'L_B' for $Ni_{0.5}Co_{0.5}Fe_{2-x}Pr_xO_4$

Figure 3 depicts the variation of hopping lengths 'L_A' and 'L_B' with Pr content 'x'. It is observed that the distance between magnetic ions increases with increase in Pr content 'x'. This behavior of hopping lengths is analogues with the behaviour of lattice constant with Pr concentration increases.

The basis of wide range of applications of ferrites is related to the variety of dopant cations that can be incorporated into the lattice of the parent ferrite. The majority of the spinel ferrites belong to the space group Fd3m with lattice parameters around 8.5 Å [12, 13]. The general equation of cation distribution in the ferrite materials can be given as,

$$\left(Fe_{\delta}^{3+}M_{1-\delta}^{2+}\right)\left[M_{\delta}^{2+}Fe_{2-\delta}^{3+}\right]O_4^{2-} \qquad 5$$

where, round bracket represents the tetrahedral – (A) site whereas the square bracket represents the octahedral – [B] site. Cation distribution over tetrahedral – (A) and octahedral – [B] sites can be obtained by using various techniques [14, 15]. In the present study X-ray diffraction data is used to estimate the cation distribution by using Bertaut method [16]. Reflection planes (220), (400), (422)

and (440) are considered as sensitive for cation distribution and are selected to calculate the selected intensity ratios (220/400), (422/440) and (440/400) by using the following relation [11],

$$\frac{I_{hkl}^{Obs.}}{I_{h'kl'}^{Obs.}} = \frac{I_{hkl}^{Calc.}}{I_{h'kl'}^{Calc.}} \qquad 6$$

The calculated and observed intensity ratios for the above pairs are given in Table 2. It is observed that the observed and calculated intensity ratios are fairly agrees with each other. The cation distribution calculated by using XRD data is given in Table 2. Table 2 clearly indicates the site preference of the cations over tetrahedral – A, and octahedral – B sites. As nickel ferrite is an example of inverse ferrite, it shows preference towards B-site only, while cobalt shows preference towards both A and B –sites but shows strong preference towards B-site. Fe^{3+} and Pr^{3+} ions distributed over both A and B sited randomly.

Table 2: Cation distribution and Intensity ratio calculations for $Ni_{0.5}Co_{0.5}Fe_{2-x}Pr_xO_4$ ferrite system.

Comp. 'x'	Cation Distribution							Intensity ratio calculations					
	A – Site			B-Site				(220/400)		(422/440)		(440/400)	
	Co	Pr	Fe	Co	Pr	Ni	Fe	Obs.	Cal.	Obs.	Cal.	Obs.	Cal.
0.0	0.1	0	0.9	0.4	0	0.5	1.100	1.365	1.240	0.220	0.210	1.912	2.020
0.025	0.1	0.01	0.89	0.4	0.015	0.5	1.085	1.323	1.276	0.220	0.212	1.903	2.065
0.050	0.1	0.02	0.88	0.4	0.030	0.5	1.070	1.308	1.305	0.210	0.213	1.633	2.109
0.075	0.1	0.03	0.87	0.4	0.045	0.5	1.055	1.341	1.334	0.205	0.216	1.804	2.135
1.0	0.1	0.04	0.86	0.4	0.060	0.5	1.040	1.456	1.468	0.219	0.220	1.853	2.144

CONCLUSIONS:

$Ni_{0.5}Co_{0.5}Fe_{2-x}Pr_xO_4$ (with x = 0.0, 0.025, 0.050, 0.075, 0.1) ferrite nanoparticles are successfully prepared by sol-gel auto combustion method. Final sintering temperature is obtained from TG curves. The single phase cubic spinel structure of all the samples is confirmed by using XRD data. The lattice parameter increases with increase in Pr substitution. The behaviour of hopping lengths is analogues with the behaviour of lattice constant. Cation distribution suggest that, nickel shows preference towards B-site only, while cobalt shows preference towards both A and B –sites but shows strong preference towards B-site. Fe^{3+} and Pr^{3+} ions distributed over both A and B sited randomly.

REFERENCES:

[1] O. Suwalka, R. K. Sharma, V. Sebastian, N. Lakshmi, K. Venugopalan; A. study of nanosized Ni substituted Co-Zn ferrite prepared by coprecipitation; J. Magn. Magn. Mater; 313 (2007) 198-203.

[2] A. K. M. Zakaria, M. A. Asgar, S. G. Eriksson, F. U. Ahmed, S. M. Yunus, H. Rundlof; The study of magnetic ordering in the spinel system $Zn_xNi_{1-x}FeCrO_4$ by neutron diffraction; J. Magn. Magn. Mater 265 (2003) 311-320.

[3] J. L. Dormann, M. Nogues, M. Nogues; Magnetic structures in substituted ferrites; J. Phys. Cond. Matter. 2 (1990) 1223.

[4] S. Krupicka, P. Novak, Oxide spinels, in E. P. Wohlfarth (Ed.) Ferromagnetic Materials, Vol. 3, Nort-Holland, Amsterdam, 1982, p. 189.

[5] S. Bid, S. K. Pradhan; Characterization of crystalline structure of ball-milled nano-Ni-Zn-ferrite by Rietveld method; Mater. Chem. Phys. 84 (2004) 291-301.

[6] P. Ravindernathan, K. C. Patil; Novel solid solutions precursor method for the preparation of ultrafine Ni-Zn ferrites; J. Mater. Sci. 22 (1987) 3261-3264.

[7] H. Igarash, K. Ohazaki; Effect of porosity and grain size on the magnetic properties of NiZn ferrite; J. Am. Ceram. Soc. 60 (1977) 51-54.

[8] G. Mustafa, M. U. Islam, W. Zhang, Y. Jamil, A. W. Anwar, M. Hussain; M. Ahmed; Investigation of structural and magnetic properties of Ce^{3+} substituted nanosized Co-Cr ferrites for a variety of applications; J. Alloys. Comp. 618 (2015) 428-436.
[9] Vivek Chaaudhari, R. H. Kadam, M. L. Mane, S. E. Shirsath, A. B. Kadam, D. R. Mane J. Nanoscience and Nanotechnology 14 (2014) 1-8.
[10] R. H. Kadam, Kirti Desai, S. R. Kadam, S. E. Shirsath; Solid State Science 26 (2013) 31.
[11] R. H. Kadam, S. T. Alone, M. L. Mane, A. R. Birajdar, S. E. Shirsath; Phase evaluation of Li^+ substituted $CoFe_2O_4$ nanoparticles, their characterization and magnetic properties; J. Magn. Magn. Mater 355 (2014) 70-75
[12] M. A. Gabal, S. S. Ata-Allah; Concerning the cation distribution in $MnFe_2O_4$ synthsized through the thermal decomposition of oxalates; J. Phys. Chem. Solids 65 (2004) 995-1003.
[13] K. E. Sickafus, J. M. Wills, N. W. Grims; Structure of spinel; J. Am. Ceram. Society; 82 (1999) 3279-3292.
[14] M. K. Fayek, F. M. Sayed, S. S. Ata-Allah, M. K. Elnimer, M. F. Moustafa, Crystal, magnetic and electric behaviour of $CoMn_xFe_{2-x}O_4$ cubic ferrites; J. Mater. Sci. 27 (1992) 4813-4817.
[15] M. K. Fayek, S. S. Ata-Allah, H. S. Refai; On the cation distribution in $Ni_{1-x}Cu_xFe_{2-y}Al_yO_4$ spinels; J. App. Phys. 85 (1999) 325.
[16] J. M. R. Gonzalez, C. O. Arean, J Chem. Soc. Dalton Trans. (1985) 2155.

LBP PUBLICATION